Postprint of: Nosko O., Olofsson U., Quantification of ultrafine airborne particulate matter generated by the wear of car brake materials, Wear, Vol. 374–375 (2017), pp. 92-96, DOI: 10.1016/j.wear.2017.01.003

Quantification of ultrafine airborne particulate matter generated by the wear of car brake materials

Oleksii Nosko*, Ulf Olofsson
Department of Machine Design, KTH Royal Institute of Technology
Brinellvägen 83, Stockholm, 100 44, Sweden

The wear of car brakes is one of the main sources of airborne particulate matter in urban environments. Ultrafine wear particles are of special environmental interest since they can easily penetrate the human body through inhalation and cause various diseases. In the present study, the contribution of ultrafine particles to airborne particulate matter emitted from car brake materials was investigated under different friction conditions. Particles were generated using a pin-on-disc machine located in a sealed chamber and analysed in terms of number, volume and mass concentrations. It was found that temperature has a strong influence on the size distribution of the emitted particles. At temperatures below 200 °C, the ultrafine particles make no measurable contribution to the mass concentration of airborne particles with diameters smaller than 10 μm (PM10). However, at temperatures above 200 °C, the mass fraction of the ultrafine particles in PM10 reaches tens of percent. In general, this fraction increases with the temperature and decreases with the sliding duration. The mass contribution of ultrafine wear particles to PM10 is substantial, and it should not be neglected in environmental and tribological studies.

Keywords: pin-on-disc; brake wear; wear particles, airborne particles; ultrafine particles; PM10.

* Corresponding author. E-mail: nosko@kth.se (O. Nosko).

1. Introduction

Braking is a frequently occurring phase of the operation of a car. During this phase, brake pads are pressed against rotating brake discs, and deceleration of the car is thereby provided. The friction between the pads and discs is inevitably accompanied by the wear of the friction surfaces and the emission of wear particles to the atmosphere (Furusjö et al. [1]; Gietl et al. [2]). If a large amount of these particles get into the human body through inhalation or skin contact, this can result in various diseases (Pope III et al. [3]; Oberdörster et al. [4]). Therefore, in recent years there has been an increasing interest in the study of environmental impacts of airborne particulate matter emitted from car brakes (Gasser et al. [5]; Amato et al. [6]; Malachova et al. [7]).

Concentration of airborne particulate matter is often characterised by PM10, which indicates the mass of airborne particles with diameters smaller than 10 μm per unit volume. The studies by Garg et al. [8], Sanders et al. [9], Kukutschová et al. [10], Wahlström at al. [11], Alemani et al. [12], and Nosko et al. [13] showed that under certain friction conditions car brake materials emit ultrafine particles (with diameters below 0.1 μm), and the number concentration of these particles is several orders of magnitude higher than that of fine particles (with diameters above 0.1 μm). This implies that the mass contribution of ultrafine particles to PM10 can be considerable.

The disposition of inhaled particles in the respiratory tract depends on their sizes. Ultrafine particles reach the tiny sacs of the lungs (alveoli), and some of them may even enter the blood circulation. Fine particles are deposited mainly in the upper respiratory tract (nasal cavity, pharynx and larynx). Oberdörster [14] concluded that ‘ultrafine particles cause a greater inflammatory response than do fine particles per given mass’. Thus, the mass fraction of ultrafine particles in PM10 is critical for correct characterisation of environmental impacts of airborne wear particles. The purpose of this study was to investigate the mass fraction of ultrafine particles in PM10 generated by the wear of car brake materials.

2. Experimental

The tests were performed using the pin-on-disc machine presented schematically in Fig.1. The pin sample was a cylinder with diameter D = 10 mm. A dead weight pressed it against a horizontally positioned disc with a pressure p. The disc, with an outer diameter of 63 mm and a thickness of 6 mm, was driven by a motor. The average radius of friction was 25 mm. The temperature of the disc was measured by a chromel–alumel thermocouple. The hot junction of the thermocouple, 0.5 mm in diameter, was installed at the average friction radius at a distance of 3 mm from the friction surface.

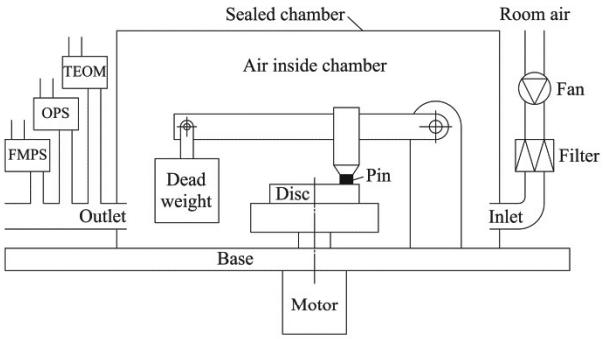

Fig.1. Schematic of the experimental pin-on-disc set-up

The pin-on-disc machine was located in a sealed chamber. The room air was drawn in by a fan and entered the chamber via a HEPA filter and an inlet, with a flow rate of 2.2 L/s. The filter removed particles from the passing air flow. The air inside the chamber picked up the particles generated by the wear of the pin sample and disc and transported them to the air outlet. This experimental set-up was proposed by Olofsson et al. [15].

The air coming out of the chamber was analysed by three aerosol measurement instruments: a TSI Fast Mobility Particle Sizer 3091 (FMPS), a TSI Optical Particle Sizer 3330 (OPS), and a Thermo Fisher Scientific Tapered Element Oscillating Microbalance 1400a (TEOM). The FMPS classifies 0.0056–0.56 μm particles into 32 stages. The stages 1 to 20, with the particle diameter range of 0.0056 to 0.1 μm, correspond to ultrafine particles. The OPS classifies 0.3–10 μm particles into 16 stages. The stages 21 to 32 of the FMPS and the stages 4 to 16 of the OPS cover particles with diameters between 0.1 and 10 μm, which will be referred to as ‘fine particles’. The TEOM measures PM10. The readings from the FMPS and OPS were sampled at 1 Hz. The PM10 signal was a moving average with a period of 5 min. The instruments were carefully calibrated.

The pin samples and disc samples were milled from passenger car brake pads and discs. The discs were cast iron. Six materials code-named M1, …, M6 were used as pin samples. M1, …, M5 are low-metallic materials representative for the European market, with phenolic resin as a binder and different reinforcements and abrasives. M6 is a non-asbestos organic material representative for the US market.

Each test lasted for 90 min and included three phases: 15 min acceleration, 45 min steady sliding, and 30 min deceleration. The sliding velocity at the average friction radius increased linearly from zero to a value v during the acceleration phase, was maintained constant in the steady sliding

phase, and decreased linearly to zero during the deceleration phase. The contact pressure p was constant for the entire test. For each of the six pin sample materials, eight tests were done, differing only as regards the load $p \times v$: (1) 0.5 MPa × 0.8 m/s; (2) 0.5 MPa × 1.6 m/s; (3) 0.5 MPa × 2.4 m/s; (4) 1 MPa × 0.8 m/s; (5) 1 MPa × 1.6 m/s; (6) 1 MPa × 2.4 m/s; (7) 1.5 MPa × 0.8 m/s; (8) 1.5 MPa × 1.6 m/s.

3. Results

Figure 2 shows the number concentrations C_{Fine} and $C_{\mathrm{Ultrafine}}$ of fine and ultrafine particles, respectively, and the disc temperature vs. time. It is seen that C_{Fine} exceeds a level of 10^3 no/cm^3. $C_{\mathrm{Ultrafine}}$ increases by several orders of magnitude at about 11 min, when the disc temperature is near 185 °C, and attains 10^7 no/cm^3. During the steady sliding phase, the disc temperature reaches a stationary value T of about 350 °C. Fig.3 shows the values of T for the tests.

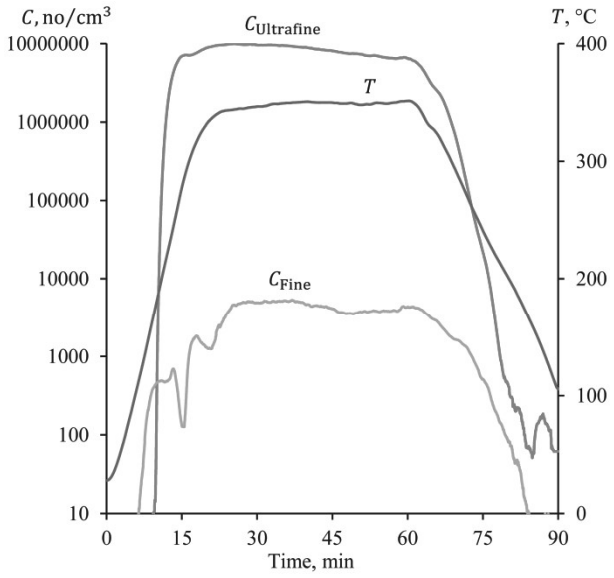

Fig.2. Particle number concentrations C_{Fine} and $C_{\mathrm{Ultrafine}}$ vs. time (M1, 1.5 MPa × 1.6 m/s) (colour online only)

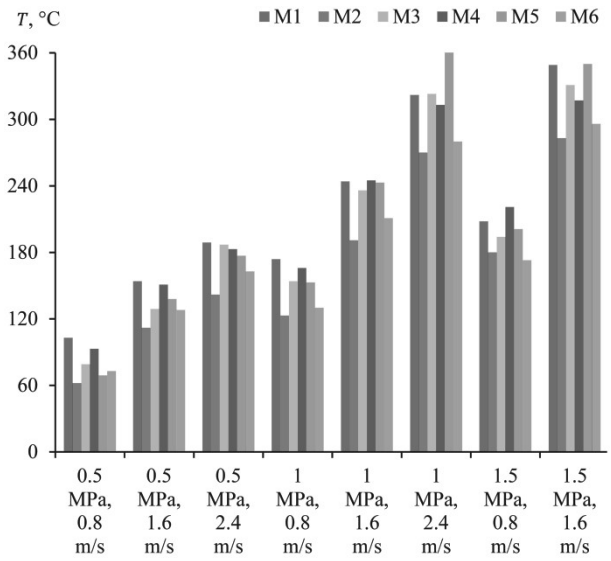

Fig.3. Stationary temperature T reached in the steady sliding phase (colour online only)

Figure 4 presents particle size distributions obtained at 10 min, i.e. before the drastic increase in $C_{\text{Ultrafine}}$, and at 60 min, which is the end of the steady sliding phase. The 10-min distribution has a peak at 0.165 μm and indicates the absence of ultrafine particles. By contrast, the 60-min distribution shows a predominance of ultrafine particles, with a peak at 0.011–0.029 μm. The particle size distributions were obtained by merging the FMPS distribution (stages 1 to 32) and the OPS stages 4 to 16, which cover together the diameter range of 0.0056 to 10 μm.

It is noteworthy that the FMPS classifies particles due to their electrical mobility diameters, while the OPS measures optical diameters. Constructing a complete size distribution using data from these two instruments generally requires application of a special alignment method based on estimates of aerosol refractive index and effective density (Hand and Kreidenweis [16]). According to the measurement data, the FMPS and OPS indicated relatively close concentrations in the overlapping diameter range 0.3 to 0.56 μm (FMPS stages 29 to 32, OPS stages 1 to 3). In most of the tests, the average difference between the concentrations in the steady sliding phase was below 35%. Therefore, no alignment method was used for simplicity in this study.

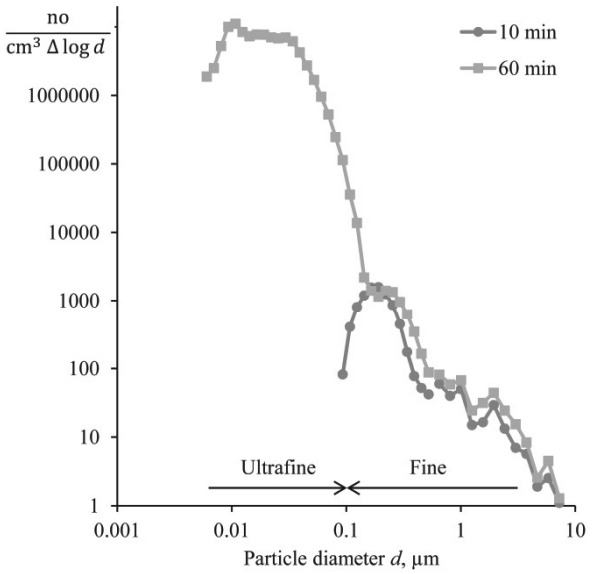

Fig.4. Particle size distributions (M1, 1.5 MPa × 1.6 m/s) (colour online only)

Assuming a spherical particle shape, one can calculate the volume concentration of particles based on their size distribution. Fig. 5 shows time dependencies of PM10, the calculated volume concentrations V_{Fine} and $V_{\mathrm{Ultrafine}}$ of fine and ultrafine particles, respectively, and the total volume concentration $V_{\mathrm{Total}} = V_{\mathrm{Fine}} + V_{\mathrm{Ultrafine}}$. During the steady sliding phase, PM10 and V_{Total} stabilise around 200 μg/m^3 and 250 μm^3/cm^3, respectively, while there is a tendency to increase in V_{Fine} and to decrease in $V_{\mathrm{Ultrafine}}$. Fig.6 shows plots $V_{\mathrm{Ultrafine}}$ vs. time for the six materials.

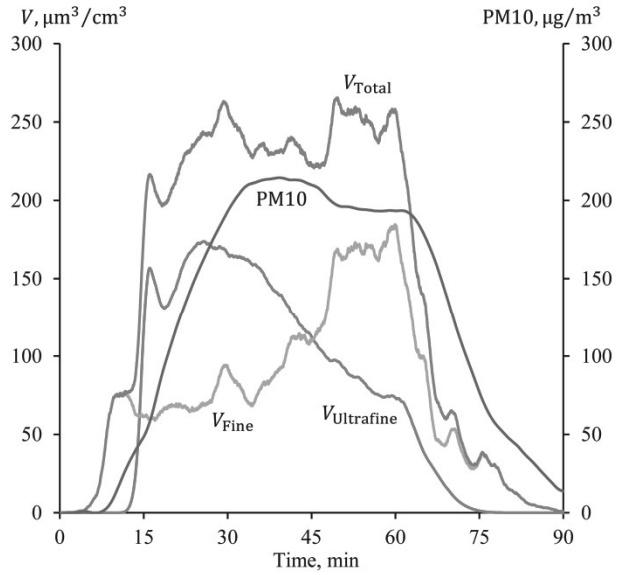

Fig.5. Particle volume concentrations V_{Fine} and $V_{\mathrm{Ultrafine}}$ and PM10 vs. time (M1, 1.5 MPa × 1.6 m/s) (colour online only)

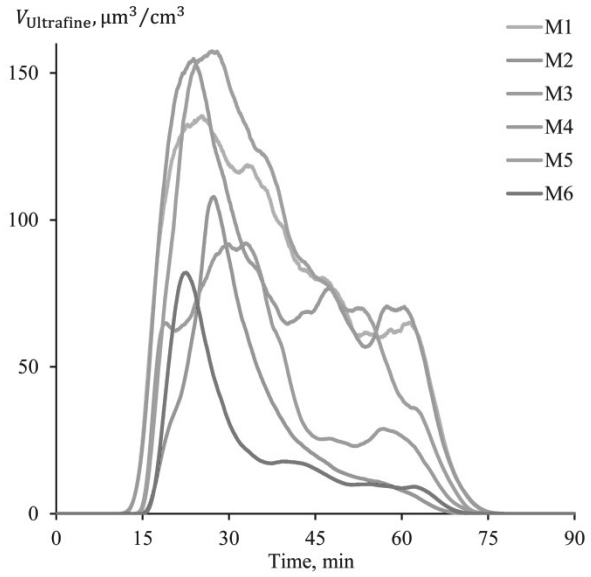

Fig.6. Ultrafine particle volume concentration $V_{\text{Ultrafine}}$ vs. time (1 MPa × 2.4 m/s) (colour online only)

Figure 7 presents the volume fraction of ultrafine particles

$$\vartheta = \frac{V_{\text{Ultrafine}}}{V_{\text{Total}}} = \frac{V_{\text{Ultrafine}}}{V_{\text{Fine}} + V_{\text{Ultrafine}}}$$

averaged in the interval 30 to 60 min. The fraction ϑ is zero at the loads of 0.5 MPa × 0.8 m/s, 0.5 MPa × 1.6 m/s, 0.5 MPa × 2.4 m/s, 1 MPa × 0.8 m/s, and 1.5 MPa × 0.8 m/s (except for M1). Fig.8 shows the relationship between ϑ and T obtained from the measurement data of Figs.3 and 7.

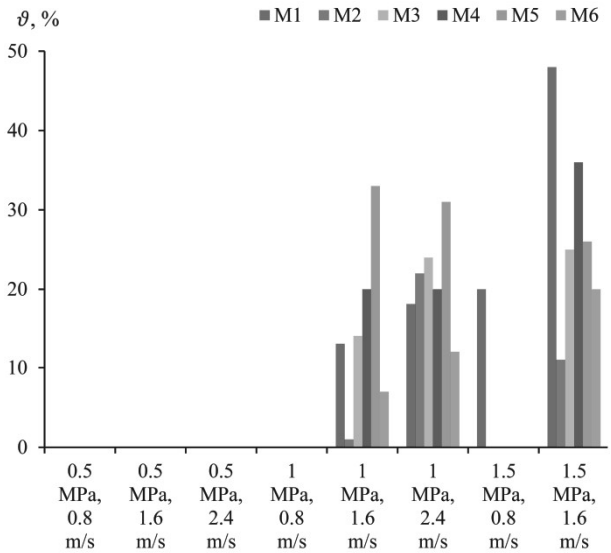

Fig.7. Volume fraction ϑ of ultrafine particles (colour online only)

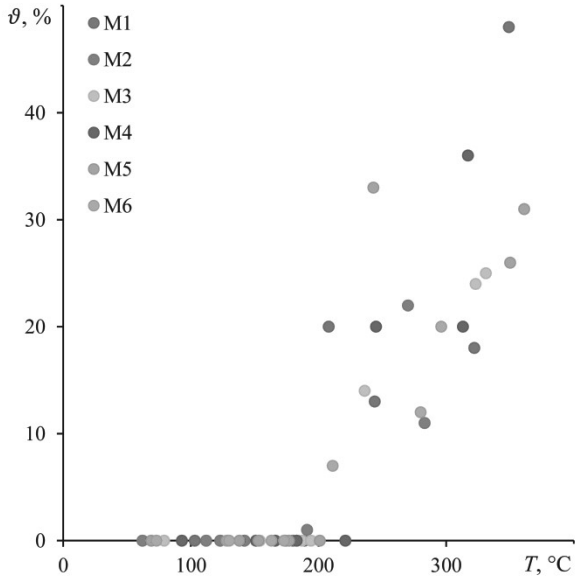

Fig.8. Relationship between the ultrafine particle volume fraction ϑ and temperature T (colour online only)

4. Discussion

Figures 2 and 4 show that 0.011–0.029 μm particles predominate in number at T > 185 ºC. Alemani et al. [12] investigated the emission rate, size distribution and elemental composition of airborne wear particles for the six materials under constant friction conditions. It was found that the emission of 0.011–0.034 μm particles intensifies at temperature 165–190 ºC, which is consistent with the results obtained in this study. It was also found [12] that the average particle material density slightly depends on the particle aerodynamic diameter in the range of 0.06 to 10 μm, which implies that the mass fraction of ultrafine particles in PM10 can be assumed equal to the volume fraction ϑ.

The data of Fig.5 allow determining the volume contributions of fine and ultrafine particles. In the interval 30 to 60 min, PM10 and V_{Total} have a relatively steady behaviour but the components of V_{Total} undergo changes: V_{Fine} increases and $V_{\mathrm{Ultrafine}}$ decreases. At 30 min $\vartheta \approx 64$ %, i.e. the ultrafine particles make bulk of the particulate matter volume. On the contrary, at 60 min $\vartheta \approx 28$ %, i.e. the fine particles predominate in volume over the ultrafine particles. The decrease in $V_{\mathrm{Ultrafine}}$ with the sliding duration is typical for the six materials, as illustrated in Fig.6.

Analysis of the data presented in Fig.7 shows that there is no correlation between ϑ and p and between ϑ and v. Of interest is the relationship between ϑ and T shown in Fig.8. At T below about 200 ºC, ϑ is negligibly small, whereas ϑ increases with T to a level of several tens of percent at T > 200 ºC.

The two 'critical' temperatures of 185 ºC and 200 ºC allow distinguishing the following temperature intervals. At T < 185 ºC both number fraction of ultrafine particles and ϑ are almost zero. Furthermore, at T between 185 and 200 ºC the ultrafine particles predominate in number but ϑ is still negligibly small. Finally, at T > 200 ºC the ultrafine particles are almost 100 % in number and ϑ is substantial.

It is important to note that the test conditions differed considerably from the real conditions of the operation of car brakes, including geometrical sizes of the friction components, sliding velocity, particle generation rate, and airflow regime. The study by Wahlström et al. [17] compared measurements of airborne particles sampled directly behind a brake pad of a passenger car and those made on the pin-on-disc set-up used in this study. It was found that despite orders of magnitude difference in the particle number concentrations, there is a good correlation between a normalised size distribution of particles emitted from the car brake and the corresponding distribution of particles generated by the pin-on-disc set-up. The particle measurements were made by a Grimm 1.109 aerosol spectrometer in the diameter range of 0.25 to 32 μm. It was thus shown that the subscale test results, including the normalised particle size distribution, can be directly related to particle emissions from full size car brakes.

Volumetric temperatures of car brake pads and discs, measured by conventional thermocouples during the braking process, are normally below 200 ºC (Garg et al. [8]). However, temperatures at the friction surfaces, determined using special measurement techniques such as an exposed thermocouple technique (Qi and Day [18]), can significantly exceed 200 ºC. The stationary temperature T measured in the disc during the steady sliding phase is most probably a close estimate of the friction surface temperature. This presumption is based on the fact (Straffelini et al. [19], Laraqi et al. [20], Yevtushenko et al. [21]) that for a pin-on-disc system, the stationary temperature in the disc is almost uniformly distributed in the vicinity of the wear track if the Peclet number $\mathrm{Pe} = Dv/k$ is of the order 10^2 and higher. Here k is the thermal diffusivity coefficient of the disc (cast irons have $k \approx 1.3 \cdot 10^{-5}$ m^2/s). For the pin-on-disc machine and load parameters used in this study, the mentioned condition is satisfied. Consequently, the 'critical' temperature of 200 ºC can be meaningful for car brakes, especially in the case of intensive braking regime.

5. Conclusions

The present study investigated the mass contribution of ultrafine particles to airborne particulate matter emitted from low-metallic and non-asbestos organic car brake materials against cast iron under

different friction conditions. Based on the experimental results, the following primary conclusions can be made:

1) Temperature has a crucial influence on the number and mass fractions of the ultrafine particles.
2) At temperatures below 200 °C, the ultrafine particles make no measurable mass contribution to PM10.
3) At temperatures above 200 °C, the mass fraction of the ultrafine particles in PM10 reaches tens of percent. This fraction generally increases with the temperature and decreases with the sliding duration.

The findings of the study indicate the significance of the mass contribution of ultrafine wear particles and the importance of its consideration in environmental studies.

Acknowledgement

The authors wish to thank Mr Mattia Alemani and Dr Vlastimil Matějka at Brembo S.p.A.; Dr Ibrahim Metinoz at the University of Trento; Mr Magnus Brydolf and Mr Billy Sjövall at Stockholm Air and Noise Analysis; Mr Peter Ahlvik at ExIS AB; Mr Peter Carlsson, Mr Yezhe Lyu and Ms Yingying Cha at KTH Royal Institute of Technology for their technical assistance.

This work was supported by the European Union Seventh Framework Programme (FP-PEOPLE-2012-IAPP) under the Rebrake Project [grant number 324385].

References

[1] Furusjö, E., Sternbeck, J., Cousins, A.P. (2007). PM10 source characterization at urban and highway roadside locations. Science of the Total Environment, 387 (1–3), 206–219.

[2] Gietl, J.K., Lawrence, R., Thorpe, A.J., Harrison, R.M. (2010). Identification of brake wear particles and derivation of a quantitative tracer for brake dust at a major road. Atmospheric Environment, 44 (2), 141–146.

[3] Pope III, C. A., Burnett, R. T., Thun, M. J., Calle, E. E., Krewski, D. et al. (2002). Lung cancer, cardiopulmonary mortality, and long-term exposure to fine particulate air pollution. The Journal of the American Medical Association, 287 (9), 1132–1141.

[4] Oberdörster, G., Maynard, A., Donaldson, K., Castranova, V., Fitzpatrick, J. et al. (2005). Principles for characterizing the potential human health effects from exposure to nanomaterials: Elements of a screening strategy. Particle and Fibre Toxicology, 2, 8.

[5] Gasser, M., Riediker, M., Mueller, L., Perrenoud A., Blank F. et al. (2009). Toxic effects of brake wear particles on epithelial lung cells in vitro. Particle and Fibre Toxicology, 6, 30.

[6] Amato, F., Cassee, F.R., Denier van der Gon, H.A.C., Gehrig, R., Gustafsson, M. et al. (2014). Urban air quality: The challenge of traffic non-exhaust emissions. Journal of Hazardous Materials, 275, 31–36.

[7] Malachova, K., Kukutschova, J., Rybkova, Z., Sezimova, H., Placha, D. et al. (2016). Toxicity and mutagenicity of low-metallic automotive brake pad materials. Ecotoxicology and Environmental Safety, 131, 37–44.

[8] Garg, B. D., Cadle, S. H., Mulawa, P. A., Groblicki, P. J. (2000). Brake wear particulate matter emissions. Environmental Science and Technology, 34 (21), 4463–4469.

[9] Sanders, P.G., Xu, N., Dalka, T.M., Maricq, M.M. (2003). Airborne brake wear debris: Size distributions, composition, and a comparison of dynamometer and vehicle tests. Environmental Science and Technology, 37 (18), 4060–4069.

[10] Kukutschová, J., Moravec, P., Tomášek, V., Matějka, V., Smolik, J. et al. (2011). On airborne nano/micro-sized wear particles released from low-metallic automotive brakes. Environmental Pollution, 159 (4), 998–1006.

[11] Wahlström, J., Olander, L., Olofsson, U. (2012). A pin-on-disc study focusing on how different load levels affect the concentration and size distribution of airborne wear particles from the disc brake materials. Tribology Letters, 46 (2), 195–204.

[12] Alemani, M., Nosko, O., Metinoz, I., Olofsson, U. (2016). A study on emission of airborne wear particles from car brake friction pairs. SAE International Journal of Materials and Manufacturing, 9 (1), 147–157.

[13] Nosko, O., Vanhanen, J., Olofsson, U. (2017). Emission of 1.3–10 nm airborne particles from brake materials, Aerosol Science and Technology, 51 (1), 91−96.

[14] Oberdörster, G. (2001). Pulmonary effects of inhaled ultrafine particles. International Archives of Occupational and Environmental Health, 74 (1), 1–8.

[15] Olofsson, U., Olander, L., Jansson, A. (2009). A study of airborne wear particles generated from a sliding contact. Journal of Tribology, 131, 044503.

[16] Hand, J.L., Kreidenweis, S.M. (2002). A new method for retrieving particle refractive index and effective density from aerosol size distribution data. Aerosol Science and Technology, 36 (10), 1012–1026.

[17] Wahlström, J., Söderberg, A., Olander, L., Olofsson, U., Jansson, A. (2010). Airborne wear particles from passenger car disc brakes: A comparison of measurements from field tests, a disc brake assembly test stand, and a pin-on-disc machine. Proceedings of the Institution of Mechanical Engineers. Part J: Journal of Engineering Tribology, 224, 179–188.

[18] Qi, H.S., Day, A.J. (2007). Investigation of disc/pad interface temperatures in friction braking. Wear, 262, 505–513.

[19] Straffelini, G., Verlinski, S., Verma, P.C., Valota, G., Gialanella, S. (2016). Wear and contact temperature evolution in pin-on-disc tribotesting of low-metallic friction material sliding against pearlitic cast iron. Tribology Letters, 62, 36.

[20] Laraqi, N., Alilat, N., Garcia de Maria, J.M., Baïri, A. (2009). Temperature and division of heat in a pin-on-disc frictional device — Exact analytical solution. Wear, 266, 765–770.

[21] Yevtushenko, A., Ukhanska, O., Chapovska, R. (1996). Friction heat distribution between a stationary pin and a rotating disc. Wear, 196, 219–225.